BELLE-CONF-0521
LP2005-156
EPS05-493

arXiv:hep-ex/0508009v1 3 Aug 2005

Measurement of Forward-Backward Asymmetry and Wilson Coefficients in $B \to K^*\ell^+\ell^-$

K. Abe,[9] K. Abe,[47] I. Adachi,[9] H. Aihara,[49] K. Aoki,[23] K. Arinstein,[2] Y. Asano,[54]
T. Aso,[53] V. Aulchenko,[2] T. Aushev,[13] T. Aziz,[45] S. Bahinipati,[5] A. M. Bakich,[44]
V. Balagura,[13] Y. Ban,[36] S. Banerjee,[45] E. Barberio,[22] M. Barbero,[8] A. Bay,[19] I. Bedny,[2]
U. Bitenc,[14] I. Bizjak,[14] S. Blyth,[25] A. Bondar,[2] A. Bozek,[29] M. Bračko,[9, 21, 14]
J. Brodzicka,[29] T. E. Browder,[8] M.-C. Chang,[48] P. Chang,[28] Y. Chao,[28] A. Chen,[25]
K.-F. Chen,[28] W. T. Chen,[25] B. G. Cheon,[4] C.-C. Chiang,[28] R. Chistov,[13] S.-K. Choi,[7]
Y. Choi,[43] Y. K. Choi,[43] A. Chuvikov,[37] S. Cole,[44] J. Dalseno,[22] M. Danilov,[13] M. Dash,[56]
L. Y. Dong,[11] R. Dowd,[22] J. Dragic,[9] A. Drutskoy,[5] S. Eidelman,[2] Y. Enari,[23] D. Epifanov,[2]
F. Fang,[8] S. Fratina,[14] H. Fujii,[9] N. Gabyshev,[2] A. Garmash,[37] T. Gershon,[9] A. Go,[25]
G. Gokhroo,[45] P. Goldenzweig,[5] B. Golob,[20, 14] A. Gorišek,[14] M. Grosse Perdekamp,[38]
H. Guler,[8] R. Guo,[26] J. Haba,[9] K. Hara,[9] T. Hara,[34] Y. Hasegawa,[42] N. C. Hastings,[49]
K. Hasuko,[38] K. Hayasaka,[23] H. Hayashii,[24] M. Hazumi,[9] T. Higuchi,[9] L. Hinz,[19] T. Hojo,[34]
T. Hokuue,[23] Y. Hoshi,[47] K. Hoshina,[52] S. Hou,[25] W.-S. Hou,[28] Y. B. Hsiung,[28]
Y. Igarashi,[9] T. Iijima,[23] K. Ikado,[23] A. Imoto,[24] K. Inami,[23] A. Ishikawa,[9] H. Ishino,[50]
K. Itoh,[49] R. Itoh,[9] M. Iwasaki,[49] Y. Iwasaki,[9] C. Jacoby,[19] C.-M. Jen,[28] R. Kagan,[13]
H. Kakuno,[49] J. H. Kang,[57] J. S. Kang,[16] P. Kapusta,[29] S. U. Kataoka,[24] N. Katayama,[9]
H. Kawai,[3] N. Kawamura,[1] T. Kawasaki,[31] S. Kazi,[5] N. Kent,[8] H. R. Khan,[50]
A. Kibayashi,[50] H. Kichimi,[9] H. J. Kim,[18] H. O. Kim,[43] J. H. Kim,[43] S. K. Kim,[41]
S. M. Kim,[43] T. H. Kim,[57] K. Kinoshita,[5] N. Kishimoto,[23] S. Korpar,[21, 14] Y. Kozakai,[23]
P. Križan,[20, 14] P. Krokovny,[9] T. Kubota,[23] R. Kulasiri,[5] C. C. Kuo,[25] H. Kurashiro,[50]
E. Kurihara,[3] A. Kusaka,[49] A. Kuzmin,[2] Y.-J. Kwon,[57] J. S. Lange,[6] G. Leder,[12]
S. E. Lee,[41] Y.-J. Lee,[28] T. Lesiak,[29] J. Li,[40] A. Limosani,[9] S.-W. Lin,[28] D. Liventsev,[13]
J. MacNaughton,[12] G. Majumder,[45] F. Mandl,[12] D. Marlow,[37] H. Matsumoto,[31]
T. Matsumoto,[51] A. Matyja,[29] Y. Mikami,[48] W. Mitaroff,[12] K. Miyabayashi,[24] H. Miyake,[34]
H. Miyata,[31] Y. Miyazaki,[23] R. Mizuk,[13] D. Mohapatra,[56] G. R. Moloney,[22] T. Mori,[50]
A. Murakami,[39] T. Nagamine,[48] Y. Nagasaka,[10] T. Nakagawa,[51] I. Nakamura,[9]
E. Nakano,[33] M. Nakao,[9] H. Nakazawa,[9] Z. Natkaniec,[29] K. Neichi,[47] S. Nishida,[9]
O. Nitoh,[52] S. Noguchi,[24] T. Nozaki,[9] A. Ogawa,[38] S. Ogawa,[46] T. Ohshima,[23] T. Okabe,[23]
S. Okuno,[15] S. L. Olsen,[8] Y. Onuki,[31] W. Ostrowicz,[29] H. Ozaki,[9] P. Pakhlov,[13] H. Palka,[29]
C. W. Park,[43] H. Park,[18] K. S. Park,[43] N. Parslow,[44] L. S. Peak,[44] M. Pernicka,[12]
R. Pestotnik,[14] M. Peters,[8] L. E. Piilonen,[56] A. Poluektov,[2] F. J. Ronga,[9] N. Root,[2]
M. Rozanska,[29] H. Sahoo,[8] M. Saigo,[48] S. Saitoh,[9] Y. Sakai,[9] H. Sakamoto,[17]
H. Sakaue,[33] T. R. Sarangi,[9] M. Satapathy,[55] N. Sato,[23] N. Satoyama,[42] T. Schietinger,[19]
O. Schneider,[19] P. Schönmeier,[48] J. Schümann,[28] C. Schwanda,[12] A. J. Schwartz,[5]
T. Seki,[51] K. Senyo,[23] R. Seuster,[8] M. E. Sevior,[22] T. Shibata,[31] H. Shibuya,[46]
J.-G. Shiu,[28] B. Shwartz,[2] V. Sidorov,[2] J. B. Singh,[35] A. Somov,[5] N. Soni,[35] R. Stamen,[9]
S. Stanič,[32] M. Starič,[14] A. Sugiyama,[39] K. Sumisawa,[9] T. Sumiyoshi,[51] S. Suzuki,[39]
S. Y. Suzuki,[9] O. Tajima,[9] N. Takada,[42] F. Takasaki,[9] K. Tamai,[9] N. Tamura,[31]
K. Tanabe,[49] M. Tanaka,[9] G. N. Taylor,[22] Y. Teramoto,[33] X. C. Tian,[36] K. Trabelsi,[8]

Y. F. Tse,[22] T. Tsuboyama,[9] T. Tsukamoto,[9] K. Uchida,[8] Y. Uchida,[9] S. Uehara,[9]
T. Uglov,[13] K. Ueno,[28] Y. Unno,[9] S. Uno,[9] P. Urquijo,[22] Y. Ushiroda,[9] G. Varner,[8]
K. E. Varvell,[44] S. Villa,[19] C. C. Wang,[28] C. H. Wang,[27] M.-Z. Wang,[28] M. Watanabe,[31]
Y. Watanabe,[50] L. Widhalm,[12] C.-H. Wu,[28] Q. L. Xie,[11] B. D. Yabsley,[56] A. Yamaguchi,[48]
H. Yamamoto,[48] S. Yamamoto,[51] Y. Yamashita,[30] M. Yamauchi,[9] Heyoung Yang,[41]
J. Ying,[36] S. Yoshino,[23] Y. Yuan,[11] Y. Yusa,[48] H. Yuta,[1] S. L. Zang,[11] C. C. Zhang,[11]
J. Zhang,[9] L. M. Zhang,[40] Z. P. Zhang,[40] V. Zhilich,[2] T. Ziegler,[37] and D. Zürcher[19]

(The Belle Collaboration)

[1]*Aomori University, Aomori*
[2]*Budker Institute of Nuclear Physics, Novosibirsk*
[3]*Chiba University, Chiba*
[4]*Chonnam National University, Kwangju*
[5]*University of Cincinnati, Cincinnati, Ohio 45221*
[6]*University of Frankfurt, Frankfurt*
[7]*Gyeongsang National University, Chinju*
[8]*University of Hawaii, Honolulu, Hawaii 96822*
[9]*High Energy Accelerator Research Organization (KEK), Tsukuba*
[10]*Hiroshima Institute of Technology, Hiroshima*
[11]*Institute of High Energy Physics,*
Chinese Academy of Sciences, Beijing
[12]*Institute of High Energy Physics, Vienna*
[13]*Institute for Theoretical and Experimental Physics, Moscow*
[14]*J. Stefan Institute, Ljubljana*
[15]*Kanagawa University, Yokohama*
[16]*Korea University, Seoul*
[17]*Kyoto University, Kyoto*
[18]*Kyungpook National University, Taegu*
[19]*Swiss Federal Institute of Technology of Lausanne, EPFL, Lausanne*
[20]*University of Ljubljana, Ljubljana*
[21]*University of Maribor, Maribor*
[22]*University of Melbourne, Victoria*
[23]*Nagoya University, Nagoya*
[24]*Nara Women's University, Nara*
[25]*National Central University, Chung-li*
[26]*National Kaohsiung Normal University, Kaohsiung*
[27]*National United University, Miao Li*
[28]*Department of Physics, National Taiwan University, Taipei*
[29]*H. Niewodniczanski Institute of Nuclear Physics, Krakow*
[30]*Nippon Dental University, Niigata*
[31]*Niigata University, Niigata*
[32]*Nova Gorica Polytechnic, Nova Gorica*
[33]*Osaka City University, Osaka*
[34]*Osaka University, Osaka*
[35]*Panjab University, Chandigarh*
[36]*Peking University, Beijing*
[37]*Princeton University, Princeton, New Jersey 08544*

[38]RIKEN BNL Research Center, Upton, New York 11973
[39]Saga University, Saga
[40]University of Science and Technology of China, Hefei
[41]Seoul National University, Seoul
[42]Shinshu University, Nagano
[43]Sungkyunkwan University, Suwon
[44]University of Sydney, Sydney NSW
[45]Tata Institute of Fundamental Research, Bombay
[46]Toho University, Funabashi
[47]Tohoku Gakuin University, Tagajo
[48]Tohoku University, Sendai
[49]Department of Physics, University of Tokyo, Tokyo
[50]Tokyo Institute of Technology, Tokyo
[51]Tokyo Metropolitan University, Tokyo
[52]Tokyo University of Agriculture and Technology, Tokyo
[53]Toyama National College of Maritime Technology, Toyama
[54]University of Tsukuba, Tsukuba
[55]Utkal University, Bhubaneswer
[56]Virginia Polytechnic Institute and State University, Blacksburg, Virginia 24061
[57]Yonsei University, Seoul

Abstract

We report a measurement of the ratios of Wilson coefficients A_9/A_7 and A_{10}/A_7 in $B \to K^*\ell^+\ell^-$. The result is obtained from a data sample containing 386 million $B\bar{B}$ pairs that was collected at the $\Upsilon(4S)$ resonance with the Belle detector at the KEKB asymmetric energy e^+e^- collider.

PACS numbers: 13.20.He, 11.30.Hv

Flavor-changing neutral current (FCNC) $b \to s$ processes are forbidden at tree level in the Standard Model (SM); rather, they proceed at a low rate via loop or box diagrams. If additional diagrams with non-SM particles contribute to such a decay, their amplitudes will interfere with the SM amplitudes and thereby modify the decay rate as well as other properties. This feature makes FCNC processes an ideal place to search for new physics.

To evaluate the new physics contributions in $b \to s$ processes, Wilson coefficients are used [1]. These coefficients parameterize the strength of the short distance interaction. If new physics contributes to the $b \to s$ processes, the relevant coefficients will deviate from the SM values. For electroweak penguin decays, the effective Wilson coefficients $C_7^{\rm eff}$, $C_9^{\rm eff}$ and $C_{10}^{\rm eff}$ appear in the partial decay width. A next-to-next-to-leading order (NNLO) calculation for these effective coefficients has many correction terms [2], so leading coefficients A_7, A_9 and A_{10} are usually used for the evaluation.

Measurements of the radiative penguin decay $B \to X_s\gamma$ [3, 4, 5], which are consistent with the SM prediction, strongly constrain the magnitude—but not the sign—of the Wilson coefficient A_7. This is an important constraint; however, non-SM contributions can change the sign of A_7 without changing the $B \to X_s\gamma$ branching fraction [6].

The $b \to s\ell^+\ell^-$ process is promising from this point of view, since not only the photonic penguin diagram but also the Z-penguin and box diagrams contribute to this decay mode. As a result, we can determine the relative signs of the Wilson coefficients A_7, A_9 and A_{10} as well as their absolute values. The first observations of $B \to K\ell^+\ell^-$, $B \to K^*\ell^+\ell^-$ and inclusive $B \to X_s\ell^+\ell^-$ decays were reported by the Belle Collaboration [7, 8, 9]. The measured branching fractions of these decay modes [7, 8, 9, 10, 11] were used to exclude a large area of the allowed region in the A_9-A_{10} plane [12, 13, 14]. However, the determination of the relative sign of A_7 to A_9 or A_{10} (as well as A_9 and A_{10}) requires precise measurements of differential branching fraction and the forward-backward asymmetry as functions of q^2 in these decay modes [15]. As shown in Fig. 1, the distributions are quite sensitive to the choice of Wilson coefficients.

The first measurement of the forward-backward asymmetry in $B \to K^{(*)}\ell^+\ell^-$ was reported by the Belle Collaboration [16]. The result for $B \to K^*\ell^+\ell^-$ is consistent with both the SM case and the case of a flipped sign for A_7A_{10}, however a quantitative evaluation in terms of Wilson coefficients has not been done yet.

In this paper, we present preliminary results of a measurement of Wilson coefficients in $B \to K^*\ell^+\ell^-$ using data produced in e^+e^- annihilation at the KEKB asymmetric collider [17] and collected with the Belle detector. The data sample corresponds to 357 fb^{-1} taken at the $\Upsilon(4S)$ resonance and contains approximately 386 million $B\overline{B}$ pairs. As a control sample, we also study the $B^+ \to K^+\ell^+\ell^-$ mode which has very small forward-backward asymmetry regardless of the existence of new physics [18]. Here and throughout the paper, the inclusion of charge conjugate modes is implied.

The Belle detector is a large-solid-angle magnetic spectrometer that consists of a silicon vertex detector (SVD), a 50-layer central drift chamber (CDC), an array of aerogel threshold Čerenkov counters (ACC), a barrel-like arrangement of time-of-flight scintillation counters (TOF), and an electromagnetic calorimeter comprised of CsI(Tl) crystals (ECL) located inside a super-conducting solenoid coil that provides a 1.5 T magnetic field. An iron flux-return located outside of the coil is instrumented to detect K_L^0 mesons and to identify muons (KLM). The detector is described in detail elsewhere [19]. Two inner detector configurations were used. A 2.0 cm beampipe and a 3-layer silicon vertex detector was used for the first 140 fb^{-1} data sample (DS-I) containing 152 million $B\bar{B}$ pairs, while a 1.5 cm beampipe, a 4-

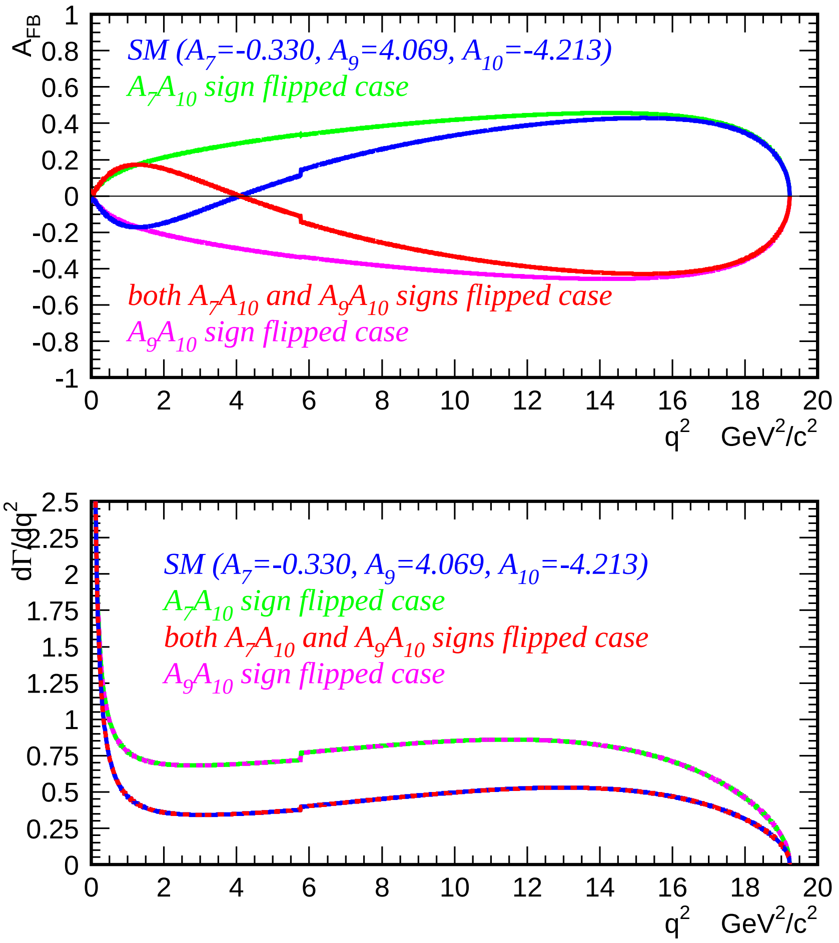

FIG. 1: Expected forward-backward asymmetry and q^2 distributions for several input parameters. The discontinuity at 5.5 GeV/c^2 is due to the imperfect matching between full and partial NNLO calculations.

layer silicon detector and a small-cell inner drift chamber were used to record the remaining 217 fb^{-1} data sample (DS-II) containing 234 million $B\bar{B}$ pairs [20].

In this analysis, primary charged tracks—except for the daughters from $K_S^0 \to \pi^+\pi^-$ decays—are required to have impact parameters relative to the interaction point of less than 5.0 cm along the z axis (aligned opposite the positron beam) and less than 0.5 cm in the $r\phi$ plane that is transverse to this axis. This requirement reduces the combinatorial background from photon conversion, beam-gas and beam-wall events.

Charged tracks are identified as either kaons or pions by a likelihood ratio based on the CDC specific ionization, time-of-flight information and the light yield in the ACC. This classification is superseded for a track that is identified as an electron or for a pion-like track that is identified as a muon. Electrons are identified from the ratio of shower energy of the matching ECL cluster to the momentum measured by the CDC, the transverse shower shape of this cluster, the specific ionization in the CDC and the ACC response. We require that the electron momentum be greater than 0.4 GeV/c to reach the ECL. Muons are identified by their penetration depth and transverse scattering in the KLM. The muon momentum is required to exceed 0.7 GeV/c. The muon identification criteria are more stringent for momenta below 1.0 GeV/c to suppress misidentified hadrons. We also apply a kaon veto for electron and muon candidates.

Photons are selected from isolated neutral clusters in the ECL with energy greater than 50 MeV and a shape that is consistent with an electromagnetic shower. Neutral pion candidates are reconstructed from pairs of photons, and are required to have an invariant mass within 10 MeV/c^2 of the nominal π^0 mass and a laboratory momentum greater than 0.1 GeV/c. The pion momentum is recalculated by constraining the invariant mass to the nominal π^0 mass. K_S^0 candidates are reconstructed from oppositely charged pions that have invariant masses within 15 MeV/c^2 of the nominal K_S^0 mass. We impose additional criteria based on the radial impact parameters of the pions (δr), the distance of closest approach of the pions along the beam direction (δz), the distance of the vertex from the interaction point (l), and the azimuthal angle difference between the vertex direction and the K_S^0 momentum direction ($\delta\phi$). These variables are combined as follows: for $p_{K_S^0} < 0.5$ GeV/c, we require $\delta z < 8$ mm, $\delta r > 0.5$ mm, and $\delta\phi < 0.3$ rad; for 0.5 GeV/$c < p_{K_S^0} < 1.5$ GeV/c, we apply $\delta z < 18$ mm, $\delta r > 0.3$ mm, $\delta\phi < 0.1$ rad, and $l > 0.8$ mm; and for $p_{K_S^0} > 1.5$ GeV/c, we impose $\delta z < 24$ mm, $\delta r > 0.2$ mm, $\delta\phi < 0.03$ rad, and $l > 2.2$ mm.

K^* candidates are formed by combining a kaon and a pion: $K^+\pi^-$, $K_S^0\pi^+$ or $K^+\pi^0$. The K^* invariant mass is required to lie within 75 MeV/c^2 of the nominal K^* mass. For modes involving neutral pions, combinatorial backgrounds are reduced by the additional requirement $\cos\theta_{\rm hel} < 0.8$, where $\theta_{\rm hel}$ is defined as the angle between the opposite of the B momentum and the kaon momentum direction in the K^* rest frame.

B candidates are reconstructed from a $K^{(*)}$ candidate and an oppositely-charged lepton pair. If a photon with energy less than 500 MeV is found in the 50 mrad cone along the electron or positron momentum direction, we add the four momentum of the bremsstrahlung photon to the di-electron system. We use two variables defined in the CM frame to select B candidates: the beam-energy constrained mass $M_{\rm bc} = \sqrt{{E^*_{\rm beam}}^2 - {p^*_B}^2}$ and the energy difference $\Delta E = E^*_B - E^*_{\rm beam}$, where p^*_B and E^*_B are the measured momentum and energy, respectively, of the B candidate, and $E^*_{\rm beam}$ is the beam energy [21]. When multiple candidates are found in an event, we select the candidate with the smallest value of $|\Delta E|$.

Backgrounds from $B \to J/\psi(\psi')K^{(*)}$ are rejected using the dilepton invariant mass. The veto windows are defined as

$$
\begin{array}{ll}
-0.25\ {\rm GeV}/c^2 < M_{ee} - M_{J/\psi} < 0.07\ {\rm GeV}/c^2 & \text{for } K^* \text{ modes} \\
-0.20\ {\rm GeV}/c^2 < M_{ee} - M_{J/\psi} < 0.07\ {\rm GeV}/c^2 & \text{for } K \text{ modes} \\
-0.20\ {\rm GeV}/c^2 < M_{ee} - M_{\psi'} < 0.07\ {\rm GeV}/c^2 & \text{for } K^* \text{ and } K \text{ modes} \\
-0.15\ {\rm GeV}/c^2 < M_{\mu\mu} - M_{J/\psi} < 0.08\ {\rm GeV}/c^2 & \text{for } K^* \text{ modes} \\
-0.10\ {\rm GeV}/c^2 < M_{\mu\mu} - M_{J/\psi} < 0.08\ {\rm GeV}/c^2 & \text{for } K \text{ modes} \\
-0.10\ {\rm GeV}/c^2 < M_{\mu\mu} - M_{\psi'} < 0.08\ {\rm GeV}/c^2 & \text{for } K^* \text{ and } K \text{ modes}
\end{array}
$$

If a bremsstrahlung photon is found, we reapply the above vetoes with the invariant mass calculated including this photon, to reject the background $J/\psi(\psi') \to e^+e^-\gamma(\gamma)$. For $K^*e^+e^-$ modes, $B \to J/\psi\, K$ can be a background if a bremsstrahlung photon is missed and a pion from the other B meson in the event is included. We suppress this background by the following prescription: the included pion is discarded and an unobserved bremsstrahlung photon is added with a direction parallel to the electron or positron and an energy that gives $\Delta E = 0$ for the B candidate. If the dilepton mass and the beam-energy constrained mass are consistent with a $B \to J/\psi\, K$ event, the candidate is vetoed.

We suppress background from photon conversions and π^0 Dalitz decays by requiring the di-electron mass to satisfy $M_{e^+e^-} > 0.14$ GeV/c^2. This cut eliminates possible peaking background from $B \to K^*\gamma$ and $B \to K^{(*)}\pi^0$.

Background from continuum $q\overline{q}$ events is suppressed using event topology. Continuum events have a jet-like shape while $B\overline{B}$ events have a spherical shape in the center-of-mass frame. A Fisher discriminant $\mathcal{F}$ [22] is calculated from the energy flow in 9 cones along the B candidate sphericity axis and the normalized second Fox-Wolfram moment R_2 [23]. We combine this with the cosine of the polar angle $\cos\theta^*_B$ of the B meson flight direction and the cosine of the polar angle $\cos\theta^*_{\rm sph}$ of the B meson sphericity axis to define likelihoods $\mathcal{L}_{\rm sig}$ and $\mathcal{L}_{\rm cont}$ for signal and continuum background, respectively, and then cut on the likelihood ratio $\mathcal{R}_{\rm cont} = \mathcal{L}_{\rm sig}/(\mathcal{L}_{\rm sig} + \mathcal{L}_{\rm cont})$. For the muon mode, $|\cos\theta^*_{\rm sph}|$ is not used since its distribution is nearly the same for signal and continuum within the detector acceptance.

The dominant background from $B\overline{B}$ events is due to semileptonic B decays. The missing energy of the event, $E_{\rm miss} = 2E^*_{\rm beam} - E^*_{\rm vis}$ where $E^*_{\rm vis}$ is a total visible energy in the event, is used to suppress this background since the undetected neutrinos carry away a substantial amount of energy. The B meson flight angle, $\cos\theta^*_B$, is also used to suppress combinatorial background in $B\overline{B}$ events. We combine $E_{\rm miss}$ and $\cos\theta^*_B$ into signal and $B\overline{B}$-background likelihoods and cut on the likelihood ratio $\mathcal{R}_{B\overline{B}}$, defined similarly to $\mathcal{R}_{\rm cont}$.

The signal box is defined as $|M_{\rm bc} - m_B| < 0.008$ GeV/c^2 for both lepton modes and -0.055 GeV$< \Delta E < 0.035$ GeV ($|\Delta E| < 0.035$ GeV) for the electron (muon) mode. We make distinct selections on $\mathcal{R}_{\rm cont}$ and $\mathcal{R}_{B\overline{B}}$ for each decay mode to optimize the sensitivity for the region with q^2 less than 6 GeV/c^2.

To determine the signal yield, we perform an unbinned maximum-likelihood fit to the $M_{\rm bc}$ distribution of events with $M_{\rm bc} > 5.2$ GeV/c^2 and -0.055 GeV$< \Delta E < 0.035$ GeV ($|\Delta E| < 0.035$ GeV) for the electron (muon) mode. We consider the signal, three cross-feed and four background components. The cross-feed components are correctly and incorrectly flavor tagged $K^*\ell^+\ell^-$ events ("cfcf" and "ifcf", respectively) and $b \to s\ell^+\ell^-$ processes other than $K^*\ell^+\ell^-$ ($X_s\ell^+\ell^-$ events). The four background components are dilepton background, $K^*\ell^\pm h^\mp$ background, $K^*h^+h^-$ background and ψ background, where h refers to a pion or a kaon. The dominant components in the signal box are signal and dilepton background. For the muon mode, $K^*\ell^\pm h^\mp$ background is sub-dominant. The ratio of $K^*\ell^\pm h^\mp$ to dilepton background is about 0.24 and 0.12 for muon and electron modes, respectively.

The expected number of signal events is calculated as a function of $M_{\rm bc}$ using a Gaussian signal distribution plus background functions. The mean and the width of the signal Gaussian are determined using observed $J/\psi K^{(*)}$ events. A MC study shows that the width has no dependence on the dilepton invariant mass. The shape and normalization of cross-feed events are parameterized by a Gaussian and an ARGUS function [24] based on MC samples.

The background from semileptonic decays is parameterized by an ARGUS function. The shape of the backgrounds are determined from large $B\bar{B}$ and continuum MC samples in which each event contains at least one oppositely charged lepton pair. The shape parameter obtained from MC is consistent with that taken from a data sample of $B \to K^{(*)}e^\pm\mu^\mp$ candidates. Since the $M_{\rm bc}$ shape for $K^*\ell^\pm h^\mp$ background is similar to that for the dilepton background, we use the same shape function. The residual background from J/ψ and ψ' mesons that cannot be removed by the $\psi^{(\prime)}$ veto windows is estimated from a large MC sample of J/ψ and ψ' inclusive events and parameterized by an ARGUS function and a Gaussian. The background contribution due to misidentification of hadrons as leptons is parameterized by another ARGUS function and a Gaussian. The ARGUS function represents the combinatorial background while the Gaussian represents the component that forms a peak in the $M_{\rm bc}$ distribution. The shape and normalization of this background are fixed using the $B \to K^{(*)}h^+h^-$ data sample (where h refers to a pion or kaon). All $K^{(*)}h^+h^-$ combinations are weighted by the momentum- and polar angle-dependent probability of misidentifying $K^{(*)}h^+h^-$ as $K^{(*)}\ell^+\ell^-$. This study yields 3.8 ± 0.4 and 2.5 ± 0.3 peaking events in the signal box for Kh^+h^- and $K^*h^+h^-$, respectively. Other backgrounds with misidentified leptons are negligible. The probability density function(PDF) for the $M_{\rm bc}$ fit is expressed as follows:

$$\begin{aligned} P(M_{\rm bc}) &= f_{\rm sig}G_{\rm sig}(M_{\rm bc}) \\ &+ f_{\rm sig}f_{\rm cfcf}\left(f^G_{\rm cfcf}G_{\rm cfcf}(M_{\rm bc}) + (1-f^G_{\rm cfcf})A_{\rm cfcf}(M_{\rm bc})\right) \\ &+ f_{\rm sig}f_{\rm ifcf}\left(f^G_{\rm ifcf}G_{\rm ifcf}(M_{\rm bc}) + (1-f^G_{\rm ifcf})A_{\rm ifcf}(M_{\rm bc})\right) \\ &+ f_{X_s\ell\ell}\left(f^G_{X_s\ell\ell}G_{X_s\ell\ell}(M_{\rm bc}) + (1-f^G_{X_s\ell\ell})A_{X_s\ell\ell}(M_{\rm bc})\right) \\ &+ f_{\rm dilep}A_{\rm dilep}(M_{\rm bc}) \\ &+ f_{K^*hh}\left(f^G_{K^*hh}G_{K^*hh}(M_{\rm bc}) + (1-f^G_{K^*hh})A_{K^*hh}(M_{\rm bc})\right) \\ &+ f_{\psi}\left(f^G_{\psi}G_{\psi}(M_{\rm bc}) + (1-f^G_{\psi})A_{\psi}(M_{\rm bc})\right), \end{aligned} \tag{1}$$

where f is the fraction of each of signal and backgrounds, G is a Gaussian and A is an ARGUS function. The $f_{\rm sig}$ and $f_{\rm dilep}$ are floated in the fit.

Figure 2 shows the fit result. We obtain 96.0 ± 12.0 and 113.6 ± 13.0 signal events for $K^+\ell^+\ell^-$ and $K^*\ell^+\ell^-$, respectively. Table I summarizes the signal yield for each subdecay mode.

Mode	Signal yield
$K^+e^+e^-$	46.6 ± 8.7
$(K^+\pi^-)^{*0}e^+e^-$	22.4 ± 7.0
$(K^0_S\pi^+)^{*+}e^+e^-$	10.9 ± 4.4
$(K^+\pi^0)^{*+}e^+e^-$	5.8 ± 4.0
$K^+\mu^+\mu^-$	49.4 ± 8.2
$(K^+\pi^-)^{*0}\mu^+\mu^-$	56.6 ± 8.8
$(K^0_S\pi^+)^{*+}\mu^+\mu^-$	7.7 ± 4.0
$(K^+\pi^0)^{*+}\mu^+\mu^-$	10.2 ± 4.1

TABLE I: Signal yields obtained from the $M_{\rm bc}$ fit. The errors are statistical only.

To extract Wilson coefficients, we perform an unbinned maximum likelihood fit to the normalized double differential decay width $(1/\Gamma)d\Gamma/dq^2d\cos\theta$ for $B \to K^*\ell^+\ell^-$ [25], where $\cos\theta$ is the cosine of the angle between negative (positive) charged lepton and B^0 or B^+ ($\overline{B}^0$ or B^-) meson momenta in the dilepton rest frame. The forward-backward asymmetry is defined as

$$A_{\rm FB}(q^2) = \frac{\Gamma(q^2, \cos\theta > 0) - \Gamma(q^2, \cos\theta < 0)}{\Gamma(q^2, \cos\theta > 0) + \Gamma(q^2, \cos\theta < 0)}. \tag{2}$$

We fix all parameters in the $C_i^{\rm eff}$ to be SM values except the leading coefficients A_7, A_9 and A_{10}. In the SM at renormalization scale $\mu = 2.5$ GeV, the values of the leading coefficients are

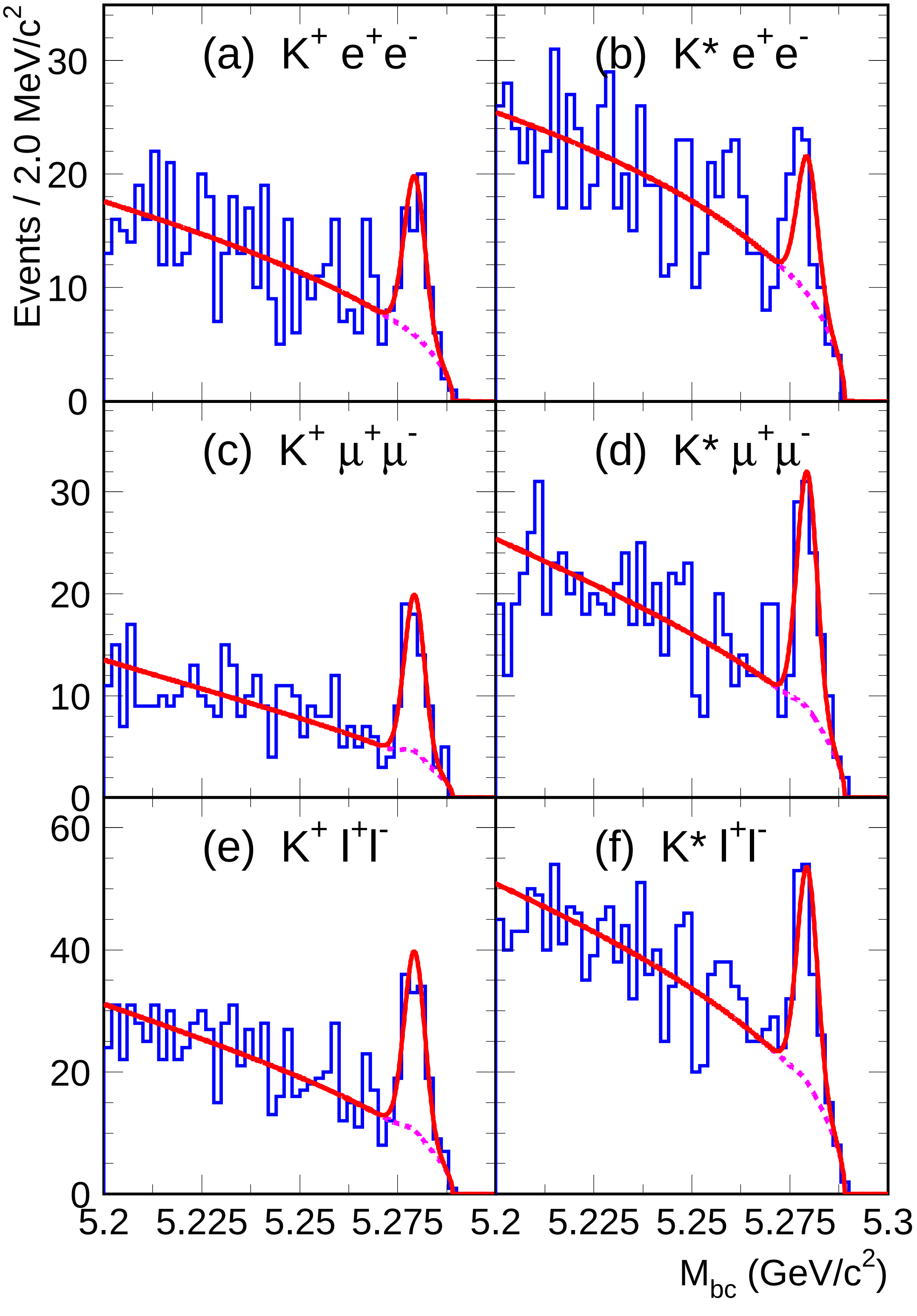

FIG. 2: $M_{\rm bc}$ distributions for (a) $B \to K^+e^+e^-$, (b) $B \to K^*e^+e^-$, (c) $B \to K^+\mu^+\mu^-$, (d) $B \to K^*\mu^+\mu^-$, (e) $B \to K^+\ell^+\ell^-$ and (f) $B \to K^*\ell^+\ell^-$ samples. The solid and dashed curves are the fit results of the total and background contributions.

$A_7 = -0.330$, $A_9 = 4.069$ and $A_{10} = -4.213$ [2, 12]. In the double differential decay width, there are a few additional parameters to be fixed. These include the form factor parameters and the bottom quark mass m_b. We choose the form factor model of Ali *et al.* [12, 25] and the bottom quark mass of 4.8 GeV/c^2 for the nominal fit. The renormalization scale μ is set at 2.5 GeV as suggested by Ref. [12].

The PDF used for the fit consists of terms describing signal, cross-feeds and backgrounds:

$$\begin{aligned}
P(q^2, \cos\theta, M_{\rm bc}) \;=\;& f_{\rm sig}(M_{\rm bc})\epsilon^{\rm DS}_{\rm sig}(q^2,\cos\theta)\frac{d^2\Gamma}{dq^2 d\cos\theta}(q^2,\cos\theta; A_7, A_9, A_{10})/N^{\rm DS}_{\rm sig}(A_7, A_9, A_{10}) \\
&+\; f_{\rm cfcf}(M_{\rm bc})\epsilon_{\rm cfcf}(q^2,\cos\theta)\frac{d^2\Gamma}{dq^2 d\cos\theta}(q^2,\cos\theta; A_7, A_9, A_{10})/N_{\rm cfcf}(A_7, A_9, A_{10}) \\
&+\; f_{\rm ifcf}(M_{\rm bc})\epsilon_{\rm ifcf}(q^2,\cos\theta)\frac{d^2\Gamma}{dq^2 d\cos\theta}(q^2,-\cos\theta; A_7, A_9, A_{10})/N_{\rm ifcf}(A_7, A_9, A_{10}) \\
&+\; f_{X_s\ell\ell}(M_{\rm bc})\mathcal{P}_{X_s\ell\ell}(q^2,\cos\theta) \\
&+\; f_{\rm dilep}(M_{\rm bc})\Big\{(1-f_{K^*\ell h})\mathcal{P}_{\rm dilep}(q^2,\cos\theta) + f_{K^*\ell h}\mathcal{P}_{K^*\ell h}(q^2,\cos\theta)\Big\} \\
&+\; f_{K^*hh}(M_{\rm bc})\mathcal{P}_{K^*hh}(q^2,\cos\theta) \\
&+\; f_{\psi}(M_{\rm bc})\mathcal{P}_{\psi}(q^2,\cos\theta), \qquad (3)
\end{aligned}$$

where f and $\mathcal{P}$ are the event by event fraction and probability density function for each components, respectively. N is the normalization factor and ϵ is the efficinecy function. Each of the fractions ($f_{\rm sig}$ etc.) are determined mode by mode from the $M_{\rm bc}$ fits except $f_{K^*\ell h}$, the fraction of $K^*\ell^\pm h^\mp$ background within the dilepton background component, which is determined from the MC samples. The efficiency functions ϵ and background distributions $\mathcal{P}$ for $X_s\ell^+\ell^-$ event, dilepton background, $K^*\ell^\pm h^\mp$ background and ψ background are obtained from large MC samples. Different efficiency functions are used for DS-I and DS-II since the acceptances are slightly different. A common background PDF used for both data sets with the averaged parameters. The Wilson coefficients in the PDF for $X_s\ell^+\ell^-$ are fixed at their SM values since this background's contribution is negligibly small. The $K^*h^+h^-$ background shape $\mathcal{P}_{K^*h^+h^-}$ is obtained from $K^*h^+h^-$ data, applying momentum- and angular-dependent lepton ID fake rate corrections.

The input parameters in the fit are q^2, $\cos\theta$ and $M_{\rm bc}$. Only A_9/A_7 and A_{10}/A_7 are allowed to float in the fit. We use smoothed histograms for efficiency and dilepton background distributions, and unsmoothed histograms for other event categories. The background PDF shapes are found to agree with the the distributions in the data sideband well.

Prior to the fit, we measure the background subtracted integrated asymmetry. To check the possible bias due to the event selection, we perform the null asymmetry test with the $K\ell^+\ell^-$ control sample. We obtain

$$A_{\rm FB}^{\rm bkg-sub}(B \to K^+\ell^+\ell^-) \;=\; 0.09 \pm 0.14({\rm stat.}). \qquad (4)$$
$$(5)$$

Note that $A_{\rm FB}^{\rm bkg-sub}$ is not corrected for the q^2-dependent efficiency. The result for $B \to K^+\ell^+\ell^-$ is consistent with zero as expected (Fig.3(a)). We thus confirm that the selection criteria do not produce any bias. On the other hand, a large asymmetry is observed for $B \to K^*\ell^+\ell^-$ (Fig.3(b),(c)):

$$A_{\rm FB}^{\rm bkg-sub}(B \to K^*\ell^+\ell^-) \;=\; 0.56 \pm 0.13({\rm stat.}). \qquad (6)$$

We fit the q^2 and $\cos\theta$ distribution for $K^*\ell^+\ell^-$ with the PDF described in the previous section. Using $A_7 = -0.330$, the best fit Wilson coefficient ratios are

$$\begin{aligned} A_9/A_7 &= -15.3\,^{+3.4}_{-4.8}, \\ A_{10}/A_7 &= 10.3\,^{+5.2}_{-3.5}\,; \end{aligned} \tag{7}$$

while, with $A_7 = +0.330$, the best fit ratios are

$$\begin{aligned} A_9/A_7 &= -16.3\,^{+3.7}_{-5.7}, \\ A_{10}/A_7 &= 11.1\,^{+6.0}_{-3.9}. \end{aligned} \tag{8}$$

Figure 3 shows the fit results projected on the background-subtracted forward-backward asymmetry distribution.

We study the systematic error due to uncertainty in the physics parameters, finite q^2 resolution, efficiencies for low momentum particles and the signal fraction. We change the A_7 value within the range allowed by the branching fraction of $B \to X_s\gamma$ [26] to obtain the corresponding systematic error. The bottom quark mass m_b is varied by ±0.2 GeV. The systematic uncertainty associated with the choise of form factor model is taken from the difference in fit results using the models of Ali *et al.* and Melikhov *et al.* [27]. We ignore smearing in q^2 in the fits, although the actual resolution is about 0.7%; the effect is measured using a toy MC study. The efficiencies to find and identify low momentum particles are slightly better in MC events, so we simultaneously reduce the efficiency for pion with $p < 0.3$ GeV, electron having $p < 0.7$ GeV and muon with $p < 1.0$ GeV to obtain revised efficinecy functions for signal and background PDFs; we then refit the data with the new PDFs. The change in the fit results correspond to the systematic error associated with the identification efficinecy. The signal fraction is determined from a fit to $M_{\rm bc}$ distribution. We change the PDF shape parameters and take the difference as a systematic error: the parameters are modified by $\pm1\sigma$ for signal and dilepton background, by 100% for cross-feed events and ψ background, and 10%(40%) for $K^*h^+h^-$ background for muon(electron) modes. For the uncertainty in $K^*\ell^\pm h^\mp$ background, we change the fraction of $K^*\ell^\pm h^\mp$ to dilepton backround, $f_{K^*\ell^\pm h^\mp}$, by 20%. Table II summarizes the contributions to the systematic error. The dominant contribution is from model dependence.

source	negative A_7 solution		positive A_7 solution	
	A_9/A_7	A_{10}/A_7	A_9/A_7	A_{10}/A_7
A_7	$^{+0.29}_{-0.03}$	$^{+0.01}_{-0.03}$	$^{+0.13}_{-0.27}$	$^{+0.36}_{-0.15}$
m_b	$^{+0.69}_{-0.68}$	$^{+0.45}_{-0.46}$	±0.63	±0.42
model dependence	±0.66	±1.72	±1.04	±2.23
q^2 resolution	±0.28	±0.39	±0.28	±0.39
efficiency	±0.08	±0.03	±0.10	±0.06
signal fraction	$^{+0.43}_{-0.47}$	$^{+0.22}_{-0.33}$	$^{+0.43}_{-0.46}$	$^{+0.37}_{-0.40}$
total	$^{+1.12}_{-1.10}$	$^{+1.83}_{-1.84}$	$^{+1.33}_{-1.36}$	$^{+2.36}_{-2.34}$

TABLE II: Systematic error for each source.

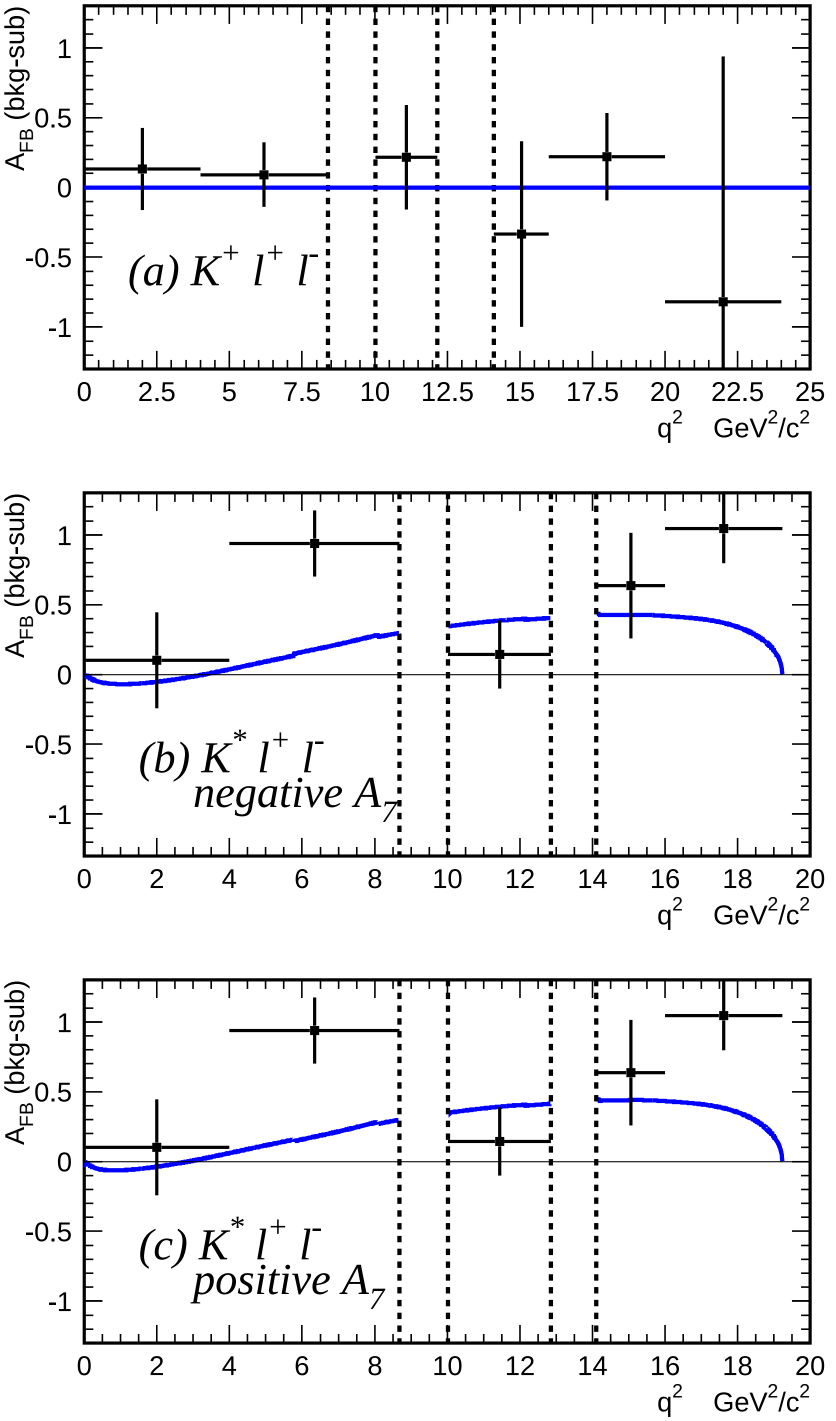

FIG. 3: Forward-backward asymmetry distributions for $K\ell^+\ell^-$ and $K^*\ell^+\ell^-$. The points show the results obtained from $M_{\rm bc}$ fits while the curves show the fit results.

The best-fit results for the Wilson coefficient ratios for negative A_7,

$$\begin{aligned} A_9/A_7 &= -15.3\,^{+3.4}_{-4.8} \pm 1.1, \\ A_{10}/A_7 &= 10.3\,^{+5.2}_{-3.5} \pm 1.8\,; \end{aligned} \tag{9}$$

and positive A_7

$$\begin{aligned} A_9/A_7 &= -16.3\,^{+3.7}_{-5.7} \pm 1.4, \\ A_{10}/A_7 &= 11.1\,^{+6.0}_{-3.9} \pm 2.4, \end{aligned} \tag{10}$$

are consistent with the SM values $A_9/A_7 = -12.3$ and $A_{10}/A_7 = 12.8$. In Fig. 4, we draw contour lines in the A_9/A_7-A_{10}/A_7 plane based on the fit likelihood smeared by systematic error (assuming Gaussian). We also calculate an interval on A_9A_{10}/A_7^2 at 95% CL for any A_7 value,

$$-1401 < A_9A_{10}/A_7^2 < -26.4. \tag{11}$$

We determine the sign of A_9A_{10} to be negative, and exclude solutions in the first or third quadrant with more than 95% CL. Both second and fourth quadrant solutions are allowed, so we cannot determine the sign of A_7A_{10} yet. Figure 5 shows the comparison between the fit results for the negative A_7 solution projected on the forward-backward asymmetry and the forward-backward asymmetry distributions for several input parameters. We exclude new physics scenarios shown by the red and magenta curves, which have positive A_9A_{10}.

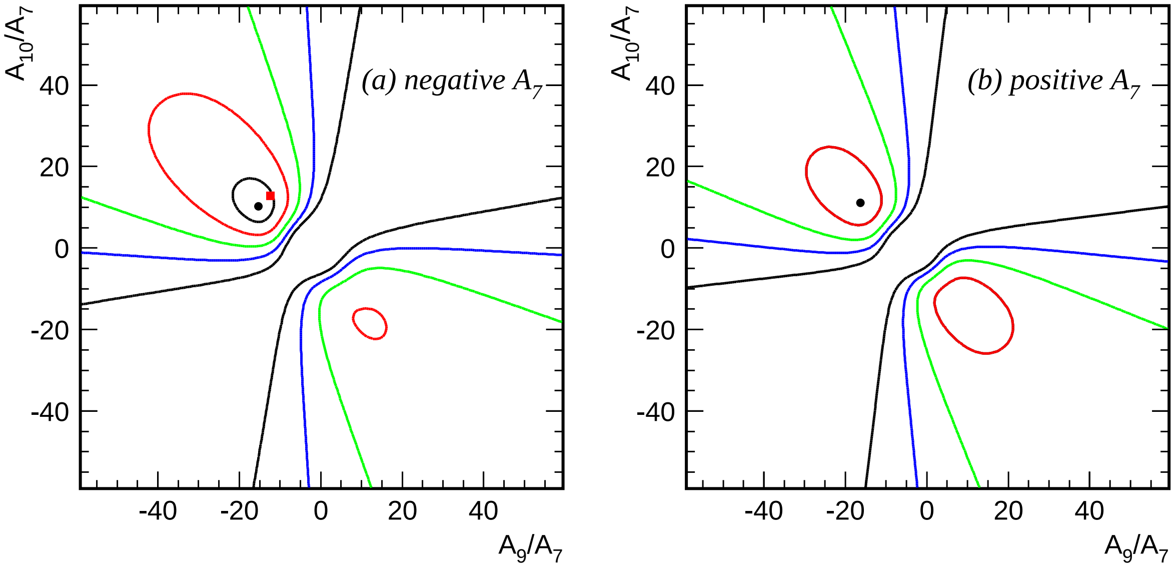

FIG. 4: Confidence level contours for negative and positive A_7. Black, red, green, blue and black curves show 1 to 5 σ contours. Black and red points show the best fit and the SM value.

In summary, we have measured for the first time the ratios of Wilson coefficients in $B \to K^*\ell^+\ell^-$ by fitting to a normalized double differential decay width. We observe a large forward-backward asymmetry in $B \to K^*\ell^+\ell^-$. The fit result is consistent with the

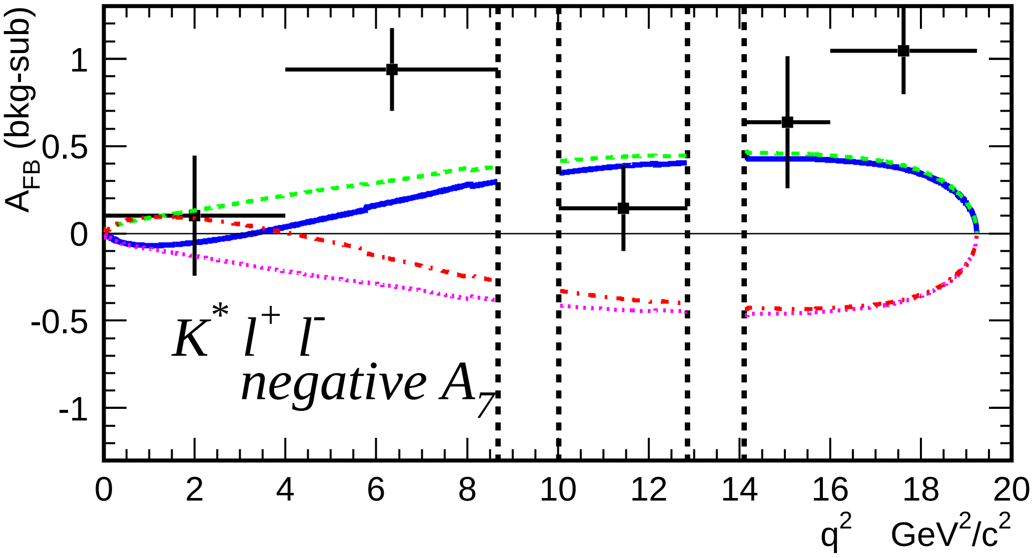

FIG. 5: Fit results for the negative A_7 solution projected to forward-backward asymmetry(solid blue) and forward-backward asymmetry curves with several input parameter including efficiency effect; A_7A_{10} sign flipped (dashed green), both A_7A_{10} and A_9A_{10} signs flipped (dash-dot red) and A_9A_{10} sign flipped(dotted magenta) to SM value. The new physics scenarios shown by the red and magenta curves are excluded.

SM prediction and also with the case where the sign of A_7A_{10} flipped. We exclude positive A_9A_{10} solutions at more than 95% CL.

We would like to thank Gudrun Hiller for her invaluable suggestions. We thank the KEKB group for the excellent operation of the accelerator, the KEK cryogenics group for the efficient operation of the solenoid, and the KEK computer group and the National Institute of Informatics for valuable computing and Super-SINET network support. We acknowledge support from the Ministry of Education, Culture, Sports, Science, and Technology of Japan and the Japan Society for the Promotion of Science; the Australian Research Council and the Australian Department of Education, Science and Training; the National Science Foundation of China under contract No. 10175071; the Department of Science and Technology of India; the BK21 program of the Ministry of Education of Korea and the CHEP SRC program of the Korea Science and Engineering Foundation; the Polish State Committee for Scientific Research under contract No. 2P03B 01324; the Ministry of Science and Technology of the Russian Federation; the Ministry of Higher Education, Science and Technology of the Republic of Slovenia; the Swiss National Science Foundation; the National Science Council and the Ministry of Education of Taiwan; and the U.S. Department of Energy.

---

[1] G. Buchalla, A. Buras and M. Lautenbacher, *Rev. Mod. Phys.* **68**, 1125 (1996) for example.
[2] H. H. Asatryan *et al. Phys. Lett.* B **507**, 162 (2001).
[3] P. Koppenburg *et al.* (Belle Collaboration), *Phys. Rev. Lett.* **93**, 061803 (2004); K. Abe *et al.*

(Belle Collaboration), *Phys. Lett.* B **511**, 151 (2001).

[4] S. Chen *et al.* (CLEO Collaboration), *Phys. Rev. Lett.* **87**, 251807 (2001).

[5] R. Barate *et al.* (ALEPH Collaboration), *Phys. Lett.* B **429**, 169 (1998).

[6] T. Besmer, C. Greub, T. Hurth. CERN-TH-2001-136, BUTP-01-12, ZU-TH-15-01, hep-ph/0105292; M. Ciuchini *et al.*, *Nucl. Phys.* B **534**, 3 (1998); C. Bobeth, M. Misiak and J. Urban, *Nucl. Phys.* B **567**, 153 (2000); F. Borzumati *et al.*, *Phys. Rev.* D **62**, 075005 (2000); T. Goto *et al.*, *Phys. Rev.* D **58**, 094006 (1998).

[7] K. Abe *et al.* (Belle Collaboration), *Phys. Rev. Lett.* **88**, 021801 (2002).

[8] A. Ishikawa *et al.* (Belle Collaboration), *Phys. Rev. Lett.* **91**, 261601 (2003).

[9] J. Kaneko *et al.* (Belle Collaboration), *Phys. Rev. Lett.* **90**, 021801 (2003).

[10] B. Aubert *et al.* (Babar Collaboration), *Phys. Rev. Lett.* **93**, 081802 (2004).

[11] M. Iwasaki *et al.* (Belle Collaboration), arXiv:hep-ex/0503044, submitted to *Phys. Rev.* D.

[12] A. Ali *et al.*, *Phys. Rev.* D **66**, 034002 (2002).

[13] E. Lunghi, arXiv:hep-ph/0210379.

[14] P. Gambino, U. Haisch and M. Misiak, *Phys. Rev. Lett.* **94**, 061803 (2005).

[15] E. Lunghi *et al.*, *Nucl. Phys.* B **568**, 120 (2000); J. L. Hewett and J. D. Wells, *Phys. Rev.* D **55**, 5549 (1997); A. Ali, G. F. Giudice and T. Mannel, *Z. Phys.* C **67**, 417 (1995); N. G. Deshpande, K. Panose and J. Trampetić, *Phys. Lett.* B **308**, 322 (1993); A. Ali, T. Mannel and T. Morozumi, *Phys. Lett.* B **273**, 505 (1991); B. Grinstein, M. J. Savage and M. B. Wise, *Nucl. Phys.* B **319**, 271 (1991); W. S. Hou, R. S. Willey and A. Soni, *Phys. Rev. Lett.* **58**, 1608 (1987).

[16] K. Abe *et al.* (Belle Collaboration), arXiv:hep-ex/0410006,

[17] S. Kurokawa and E. Kikutani, Nucl. Instr. and. Meth. A499, 1 (2003), and other papers included in this volume.

[18] D. A. Demir, K. A. Olive and M. B. Voloshin, *Phys. Rev.* D **66**, 034015 (2002).

[19] A. Abashian *et al.* (Belle Collaboration), Nucl. Instr. and Meth. A **479**, 117 (2002).

[20] Y. Ushiroda (Belle SVD2 Group), Nucl. Instr. and Meth.A **511** 6 (2003).

[21] Throughout this paper, variables denoted with an asterisk are calculated in the $\Upsilon(4S)$ rest frame.

[22] R. A. Fisher, *Ann. Eugen.* **7**, 179 (1936); M. C. Kendall and A. Stuart, *The Advanced Theory of Statistics,* Second Edition (Hafner, New York, 1968) Vol III.

[23] G. Fox and S. Wolfram, *Phys. Rev. Lett.* **41**, 1581 (1978).

[24] H. Albrecht *et al.* (ARGUS Collaboration), *Phys. Lett.* B **241**, 278 (1990).

[25] A. Ali, P. Ball, L. T. Handoko and G. Hiller, *Phys. Rev.* D **61**, 074024 (2000).

[26] Private communication with G. Hiller. She calculates an A_7 interval based on HFAG winter 2005 results [28], $0.23 < A_7 < 0.42$ and $-0.36 < A_7 < -0.19$ at 95% CL for the positive and negative solutions, respectively.

[27] D. Melikhov, N. Nikitin and S. Simula, *Phys. Lett.* B **410**, 290 (1997).

[28] Heavy Flavor Averaging Group, http://www.slac.stanford.edu/xorg/hfag.